VIBRATION CONTROL IN THE ASSEMBLY OF LARGE FLEXIBLE STRUCTURES BY TEAMS OF SPACE ROBOTS

Dimitrios Tzeranis and Steven Dubowsky

Field and Space Robotics Laboratory, Massachusetts Institute of Technology
77 Massachusetts Avenue, Cambridge MA 02139, USA
{tzeranis, dubowsky}@mit.edu

Abstract: For in-orbit assembly of future large space structures, teams of robots will be needed to manipulate large flexible structural modules while mounted on a large flexible structure. Here, the problem of planning and controlling the vibration induced in the space structures during this assembly operation is addressed. In the planning and control architecture developed, robots exploit their redundancy and use force sensors at their end-effectors to control the forces that they apply to the structures. The effectiveness of the architecture is shown through simulation results.

Keywords: Space Robotics, Force Based Control, Grasping and Manipulation.

1. INTRODUCTION

Future large space structures (LSS), such as for space solar power stations and large space telescopes, are expected to be significantly larger and more complex than the International Space Station [Oda, *et al.,* 2003]. Such space structures will need to be constructed in orbit by space robots since human extra-vehicle activity will be expensive and dangerous [Whittaker, *et al.,* 2003]. It is likely that LSS will be constructed by assembling large structural modules. These module will be carried by launch vehicles and then deployed in orbit [Oda, *et al.,* 2003]. During the construction of LSS, space robots will need to maneuver and manipulate large structural modules that are flexible and have low damping, while mounted on the LSS, Fig. 1.

This paper addresses the challenging problem of planning and controlling a team of robots so as to perform the assembly task while not exciting excessive vibration in both the module and the LSS, avoiding the application of excessive forces, and avoiding collisions that could damage the structures or the robots. This paper presents a planning and control architecture (Architecture for Minimum Vibration Manipulation - AMVM), where robots perform their manipulation tasks by first planning the forces they apply to the module and LSS, and then use force sensors to control these forces. Robots also exploit their redundancy to improve the force control performance and avoid undesirable configurations. Position errors that result from modeling errors and disturbances are compensated by modifying the planned force commands. The effectiveness of the developed architecture is shown through simulation results for a planar manipulation case.

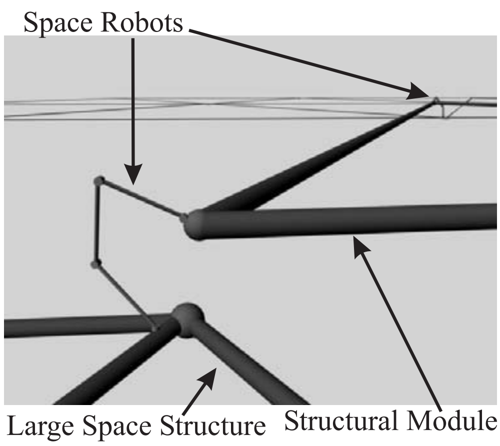

Fig. 1. Concept of using teams of robots to construct LSS by assembling large structural modules.

2. AMVM ARCHITECTURE OVERVIEW

Fig. 2 shows the assembly of a large flexible module by a team of multi-arm robots. During the assembly task, the robots use their manipulators to grasp the manipulated module and to support themselves on the LSS that is under construction. In the architecture developed here, this system is decomposed into its elements: the passive space structures and the active space robots. It is assumed that these elements interact through the forces at the robots' end-effectors and that robots have end-effector force/torque sensors that can measure these interaction forces.

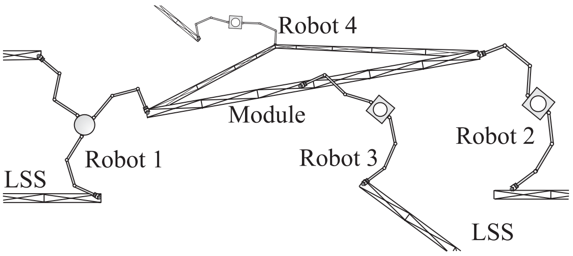

Fig. 2. Manipulation of a structural module by a team of multi-arm space robots.

The robots perform their tasks (e.g. manipulate and deform the structures) by planning and controlling their end-effector forces. This force control action is designed by first writing the dynamics of the robots and the space structures in the robots' operational space [Khatib, 1995]. The robots exploit their redundancy to improve the performance of the force control action and also to avoid collisions. The motion of each robot's redundant degrees of freedom is planned using the virtual manipulator method [Vafa and Dubowsky, 1987].

Any errors in the position of the manipulated module caused by modeling errors and external disturbances are compensated by modifying the initially planned force commands.

The actuator input for the i-th robot $\underline{\tau}_i$ is the sum of two parts, Fig. 3. The first is the robot joint torque $\underline{\tau}_{Fi}$ to control the forces that the robot applies to the space structures. The second is the joint torque $\underline{\tau}_{Mi}$ to control the robot's redundant degrees of freedom:

$$\underline{\tau}_i = \underline{\tau}_{Fi} + \underline{\tau}_{Mi} \qquad (1)$$

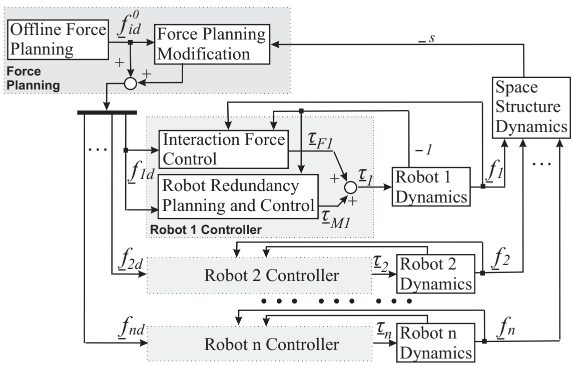

Fig. 3. Block diagram of the AMVM architecture.

3. SYSTEM DESCRIPTION

In this paper, the AMVM architecture is applied to an example of cooperative manipulation of a large flexible module by two rigid-link redundant planar robots that are mounted on the LSS, see Fig. 4. The robots manipulate the module from some initial position to a desired position in the proximity of the LSS (the module's pre-assembly position). It is assumed that the module is an order of magnitude larger than either robot. While this example is planar, the approach can be extended to the general three-dimensional case.

Each robot consists of a relatively heavy "body" and two rigid-link manipulators with three links each, Fig. 4. The robot's central body has a reaction wheel whose axis is parallel to the inertial Z axis. Each robot grasps the LSS and the module with its manipulators in such a way that it applies forces but not torques (the connection acts as a pinned joint). Each robot uses force sensors at its end-effectors to measure the forces it applies to the module and the LSS. The configuration of each robot can be described using the coordinates, see Fig. 4a.

$$\underline{x}_{ri} = \left[\underline{r}_{Gi}^T \quad \phi_i \quad \underline{\theta}_i^T\right]^T = \left[\underline{r}_{Gi}^T \quad \underline{\vartheta}_i^T\right]^T \qquad (2)$$

where $\underline{r}_{Gi}$ is the position of the robot center of mass (CM), ϕ_i is the orientation of the robot body, and $\underline{\theta}_i$ is the vector of joint angles. The subscript i=1 refers to the left robot and i=2 to the right robot in Fig. 4. The dynamics of each robot in configuration space can be written as [Papadopoulos and Dubowsky, 1991]:

$$m_{Ri}\ddot{\underline{r}}_{Gi} = -\underline{f}_{si} - \underline{f}_{bi} \qquad (3)$$

$$\underline{H}_i\ddot{\underline{\vartheta}}_i + \underline{C}_i = \underline{\tau}_i - \underline{J}_{si}^T\underline{f}_{si} - \underline{J}_{bi}^T\underline{f}_{bi} \qquad (4)$$

where m_{Ri} is the mass of robot i, $\underline{f}_{si}$ and $\underline{f}_{bi}$ are the forces applied by robot i to the module and the LSS respectively, $\underline{H}_i$ is a mass matrix and $\underline{C}_i$ contains nonlinear terms. The actuator input $\underline{\tau}_i$ consists of the torque applied by the reaction wheel to the robot body and the vector of joint torques $\underline{\tau}_{qi}$.

$$\underline{\tau}_i = \left[\tau_{wi} \quad \underline{\tau}_{qi}^T\right]^T \qquad (5)$$

The velocities of the robot end-effectors that grasp the module and the LSS can be expressed as:

$$\dot{\underline{r}}_{si} = \underline{J}_{si}^+\left[\dot{\underline{r}}_G^T \quad \dot{\underline{\vartheta}}_i^T\right]^T = \dot{\underline{r}}_G + \underline{J}_{si}\dot{\underline{\vartheta}}_i \qquad (6)$$

$$\dot{\underline{r}}_{bi} = \underline{J}_{bi}^+\left[\dot{\underline{r}}_G^T \quad \dot{\underline{\vartheta}}_i^T\right]^T = \dot{\underline{r}}_G + \underline{J}_{bi}\dot{\underline{\vartheta}}_i \qquad (7)$$

The module "rigid body" motion is described by its orientation θ_s and the inertial position $\underline{r}_{Gs}$ of its center of mass, Fig 4. The module's vibration displacement $\underline{u}_s$ is approximated by its rigid body motion and first Q free-free modes of the module through the assumed modes method [Meirovich, 1970]. It is assumed that the vibration dynamics of the module are linear and that its inertial and vibration properties are relatively well known (less than 10% error). The dynamics of the module can be written as:

$$\begin{aligned} \underline{M}_m\left[\ddot{\underline{r}}_{Gs}^T \quad \ddot{\theta}_s\right]^T &= \underline{W}_{sm}\left[\underline{f}_{s1}^T \quad \underline{f}_{s2}^T\right]^T \\ \ddot{\underline{q}}_s + 2\underline{Z}_s\underline{\Omega}_s\dot{\underline{q}}_s + \underline{\Omega}_s^2\underline{q}_s &= \underline{W}_{sv}\left[\underline{f}_{s1}^T \quad \underline{f}_{s2}^T\right]^T \end{aligned} \qquad (8)$$

where $\underline{M}_m$ is a mass matrix, $\underline{q}_s$ are the module modal coordinates, $\underline{Z}_s$ is a damping matrix, $\underline{\Omega}_s$ is a frequency matrix, and $\underline{W}_{sm}$, $\underline{W}_{sv}$ are grasp matrices [Nakamura, 1991].

The vibration displacement of the LSS at the grasping point of the i-th robot is denoted as δ_i. The dynamics of the vibration displacement of the LSS at that grasping point can be approximated as:

$$\underline{M}_{bi}\ddot{\underline{\delta}}_i + \underline{K}_{bi}\underline{\delta}_i = \underline{f}_{bi} \qquad (9)$$

where $\underline{M}_{bi}$, $\underline{K}_{bi}$ are mass and stiffness matrices. It is assumed that the force $\underline{f}_{bi}$ applied to the LSS by tobot i has no effect on the displacement of the LSS δ_j at the grasp point of robot j.

For the manipulation task considered here, it is assumed that initially the system is at rest. Robots need to plan and control the forces $\underline{f}_{si}$ they apply to the module so that it is positioned accurately and with low residual vibration. Robots also need to limit the forces $\underline{f}_{bi}$ that they apply to the LSS so that they do not excite substantial residual vibration in the LSS.

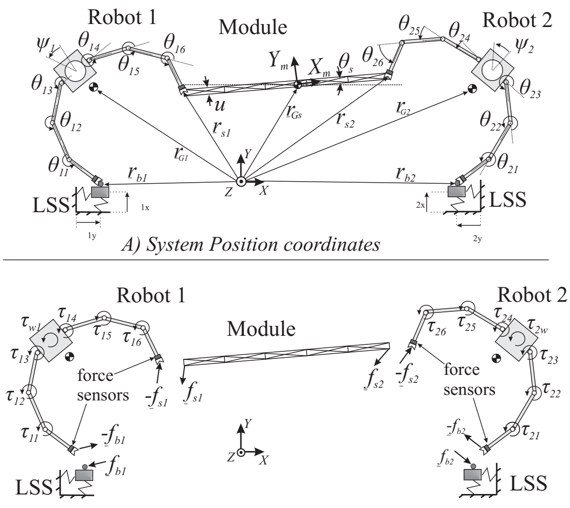

B)System Decomposition and System Force and Torque Elements

Fig. 4. Planar manipulation task.

4. THE AMVM ARCHITECTURE

4.1. Interaction Force Control

First, the AMVM architecture controls the forces that robots apply to the module and the LSS. The actuator input for each robot is expressed as:

$$\underline{\tau}_i = \underline{\tau}_{Fi} + \underline{\tau}_{Mi} = \underline{J}_{si}^T\underline{\gamma}_{si} + \underline{J}_{bi}^T\underline{\gamma}_{bi} + \underline{\tau}_{Mi} \qquad (10)$$

where $\underline{J}_{si}$, $\underline{J}_{bi}$ are defined in Eq. 6, 7 and $\underline{\gamma}_{si}$, $\underline{\gamma}_{bi}$ are 2×1 input vectors. The dynamics of the robots in operational space are found by differentiating Eq. 6, 7 and using Eq. 3, 4:

$$\begin{bmatrix} \ddot{\underline{r}}_{si} \\ \ddot{\underline{r}}_{bi} \end{bmatrix} = -\underline{M}_{Ai}^{-1}\begin{bmatrix} \underline{f}_{si} \\ \underline{f}_{bi} \end{bmatrix} + \underline{M}_{Bi}^{-1}\begin{bmatrix} \underline{\gamma}_{si} \\ \underline{\gamma}_{bi} \end{bmatrix} + \underline{f}_{misc} \qquad (11)$$

$$\underline{M}_{Ai}^{-1} = \begin{bmatrix} \underline{J}_{si}^{+} \\ \underline{J}_{bi}^{+} \end{bmatrix}\begin{bmatrix} m_{Ri}^{-1}\underline{I} & \\ & \underline{H}_i^{-1} \end{bmatrix}\begin{bmatrix} \underline{J}_{si}^{+} \\ \underline{J}_{bi}^{+} \end{bmatrix}^T \qquad (12)$$

$$\underline{M}_{Bi}^{-1} = \begin{bmatrix} \underline{J}_{si} \\ \underline{J}_{bi} \end{bmatrix}\begin{bmatrix} m_{Ri}^{-1}\underline{I} & \\ & \underline{H}_i^{-1} \end{bmatrix}\begin{bmatrix} \underline{J}_{si} \\ \underline{J}_{bi} \end{bmatrix}^T \qquad (13)$$

where $\underline{f}_{misc}$ include nonlinear terms and terms due to $\underline{\tau}_{Mi}$. The dynamics of the robots-structures system in operational space are described by combining Eq. 8, Eq. 9 and Eq. 11 to 13. Assuming that the robot joint velocities $\dot{\underline{\vartheta}}_i$ are small, the nonlinear terms can be considered as disturbances. In this case, the dynamics of each robot in operational space are dominated by its inertia, which is expressed by the matrix $\underline{M}_{Ai}$. The matrix $\underline{M}_{Ai}$ is a full 4×4 matrix which is always non-singular because $\underline{J}_{si}^{+}$, $\underline{J}_{bi}^{+}$ are nonsingular [Papadopoulos and Dubowsky, 1991]. The $\underline{M}_{Ai}$ matrix couples the dynamics of the module and the LSS. The matrices $\underline{M}_{Ai}(\underline{\vartheta}_i)$ and $\underline{M}_{Bi}(\underline{\vartheta}_i)$ are configuration dependent. While the eigenvalues of $\underline{M}_{Ai}$ $\lambda_j(\underline{M}_{Ai})$ have always finite values, there exist configurations where the maximum eigenvalue of $\underline{M}_{Bi}$ tends to infinity $\lambda_{\max}(\underline{M}_{Bi}) \to \infty$. In these configurations the robot cannot control the force that it applies to the space structures. In AMVM these configurations are avoided by exploiting robot redundancy.

The design of the force controller is done in inertial space and aims to find the inputs $\underline{\gamma}_i = \begin{bmatrix}\underline{\gamma}_{si}^T & \underline{\gamma}_{bi}^T\end{bmatrix}^T$ so that the forces $\underline{f}_i = \begin{bmatrix}\underline{f}_{si}^T & \underline{f}_{bi}^T\end{bmatrix}^T$ that robots apply to the space structures track desired force commands $\underline{f}_{id} = \begin{bmatrix}\underline{f}_{sid}^T & \underline{f}_{bid}^T\end{bmatrix}^T$.

Force controllers usually contain proportional P and integral I terms and avoid differentiation of noisy force signals. A simple linear model between the actuator efforts $\underline{\gamma}_i$ and the interaction forces $\underline{f}_i$ shows that controlling such a system by PI controllers is difficult. Since the poles and the zeros of the system are near the imaginary axis of the s plane, the PI gains must be kept low to avoid making the closed loop system unstable. However, low PI gains prevent robots from tracking reasonably fast commands and perform the manipulation task within reasonable time. The control becomes more difficult as the mass of the robots increase.

Therefore, in order to control the forces $\underline{f}_i$ using PI controllers, it is desirable that robots are relatively light and back-drivable. This can be achieved by proper robot design and by exploiting robot redundancy to avoid robot configurations that result in high operational space inertia (large $\lambda_{\max}(\underline{M}_{Ai})$). An example of such a appropriate robot design is a heavy "body" with two light manipulators, shown in Fig. 4.

The control of the forces $\underline{f}_i$ can also be improved significantly by changing the poles of the robots-space structures system. Proper placement of these poles will allow the application of higher PI gains and therefore result in increased closed loop force bandwidth. Such pole locations lie near the poles of the free-free space structures.

Assuming that each robot can exploit its redundancy to avoid certain configurations, the task-space inertia of each robot can be small compared to the inertia of the space structures. In this case the design of the force controller is simplified and based on a linearized model of the robots-structure system:

$$\dot{\underline{x}}_F = \underline{A}_F \underline{x}_F + \underline{B}_F \underline{\gamma} \qquad \underline{f} = \underline{C}_F \underline{x}_F \tag{13}$$

where $\underline{x}_F$ describes the state of the robots-structures system. The force controller consists of two parts:

$$\underline{\gamma} = \underline{\gamma}_{SF} + \underline{\gamma}_{PI} \tag{14}$$

$$\underline{\gamma}_{PI} = \underline{G}_{PI}\{\underline{f}_{id} - \underline{f}_i\} \tag{15}$$

$$\underline{\gamma}_{SF} = -\underline{K}_F \underline{x}_F \tag{16}$$

where $\underline{\gamma}_{PI}$ corresponds to the PI control action on the force tracking error $\underline{f}_{id} - \underline{f}_i$. The diagonal matrix $\underline{G}_{PI}$ contains the PI controllers for each component of $\underline{f}_i$. The input $\underline{\gamma}_{SF}$ is a state feedback control action that places the poles of the robots-structures system in proper locations of the s-plane [Gawronski 1998]. This state feedback controller could use modal information from global sensing robots [Lichter and Dubowsky 2005].

4.2. Force Planning

In the manipulation task, robots need to plan and control the forces $\underline{f}_{si}$ that they apply to the module so that the module is positioned accurately and with low residual vibration. The components ($j = X$, Y) of the desired force $\underline{f}_{sid}$ that each robot is to apply to the module are expressed as a sum of sinusoids:

$$f_{sijd}(t) = \sum_{k=1}^{M} \{a_{ijk} \sin(\omega_{pi} t)\} \tag{17}$$

The coefficients a_{ijk} are calculated offline so that the force profiles are smooth (this makes force tracking easier), the module is placed accurately and with low residual vibration. Residual vibration in the module will be low if the forces $\underline{f}_{si}$ applied to the module satisfy the following condition for all dominant vibration modes of the module [Bhat and Miu, 1990]:

$$\left\| \int_0^{\Delta t} h_i(t) e^{-s_i t} dt \right\| = 0 \tag{18}$$

where Δt is the manipulation duration, s_i is the pole location of module mode i, and $h_i(t)$ is the excitation of the module mode i due to $\underline{f}_{si}$. During the manipulation task robots also need to limit the reaction forces $\underline{f}_{bi}$ they apply to the LSS.

The calculation of the coefficients a_{ijk} (Eq. 17) is based on a model of the module. Any errors in this model or external disturbance forces (e.g. due to orbital mechanics) that are applied to the module will induce position errors. Here, the compensation of these errors is done by modifying the initial planned force commands $\underline{f}^0_{sid}$ (calculated offline) by an impedance force correction action:

$$\underline{f}_{sid} = \underline{f}^0_{sid} + \delta \underline{f}_{sid} \tag{19}$$

$$\delta \underline{f}_{sid} = \underline{W}^+_{sm}(\underline{K}_{PG}(\hat{\underline{\rho}}_s - \underline{\rho}_s) + \underline{K}_{DG}(\dot{\hat{\underline{\rho}}}_s - \dot{\underline{\rho}}_s)) \tag{20}$$

where $\underline{W}^+_{sm}$ is the pseudoinverse of $\underline{W}_{sm}$, $\underline{\rho}_s = \begin{bmatrix} \underline{r}^T_{Gs} & \theta_s \end{bmatrix}^T$ are the measured coordinates of the module's rigid body motion, and $\hat{\underline{\rho}}_s$ is the estimated values of $\underline{\rho}_s$ that would result from $\underline{f}^0_{si}$ according to the module model.

4.3. Robot Motion Planning and Control

The second part of the AMVM architecture is to plan and control each robot's redundant degrees of freedom so that the robot avoids undesirable configurations (singularities, configurations that result in high task-space inertia) and collisions.

The motion of each robot is planned based on the virtual manipulators that describe the position of its endpoints $\underline{r}_{si}$ and $\underline{r}_{bi}$ [Vafa and Dubowsky, 1987] by applying inverse kinematics algorithms to Eq. 6 and 7:

$$\begin{bmatrix} \dot{\hat{\underline{r}}}_{si} - \dot{\hat{\underline{r}}}_{Gi} \\ \dot{\hat{\underline{r}}}_{bi} - \dot{\hat{\underline{r}}}_{Gi} \end{bmatrix} = \begin{bmatrix} \underline{J}_{si} \\ \underline{J}_{bi} \end{bmatrix} \dot{\underline{\vartheta}}_{id} \tag{21}$$

where the estimated motions of the robot CM $\hat{\underline{r}}_{Gi}$ and the robot endpoints $\hat{\underline{r}}_{si}$, $\hat{\underline{r}}_{bi}$ are calculated from the commands $\underline{f}_{sid}$.

Each robot can control in closed loop the forces it applies to the flexible space structures, the attitude of its central body ϕ_i and the motion of its redundant joint angles. The actuator input $\underline{\tau}_{Mi}$ to control the motion of the i-th robot redundant degrees of freedom is expressed as:

$$\underline{\tau}_{Mi} = \underline{\tau}_{FFi} + \underline{\tau}_{PDi} \tag{22}$$

where $\underline{\tau}_{FFi}$ is a feed-forward term (calculated using the robot dynamics described by Eq. 3, 4) and $\underline{\tau}_{PDi}$ is a PD control action on the robot redundant degrees of freedom.

5. SIMULATION RESULTS

5.1. System Description

Here Matlab/Simulink simulation results are provided for the manipulation of a large flexible beam by two planar redundant robots that are mounted on a LSS, see Fig. 4. The properties of the robots and the beam are given in Tables 1 and 2. It is assumed that the LSS is much stiffer in the X direction than in the Y direction. The dynamics of the LSS (Eq. 9) in the Y direction are modelled by a mass m_B of 2000 kg and a spring rate k_B of 20 N/m. Robots do not apply torques to the LSS therefore they induce vibration in the LSS only through the forces $\underline{f}_{bi}$ they apply to the LSS.

Table 1: Robot properties

Link length [m]	[3, 3, 3, 2, 3, 3, 3]
Link mass [kg]	[18,18,18,242,18,18, 18]
Reaction wheel mass [kg]	40
Reaction wheel inertia [kg·m^2]	20

Table 2: Beam properties

Length [m]:	200
Young's modulus [GPa]	0.16
Cross section [m]	1×1
Linear density [kg/m]:	3
Low vibr. modes [Hz]	f_1=0.20, f_2=0.54, f_3=1.04

The design of the robot controller is based on the beam motion specifications given in Table 3. The state-space controller of Eq. 16 takes into consideration only the first two flexible modes of the beam. The gain $\underline{K}_F$ is chosen so that the poles of the robots-beam system are placed at -0.6 ±1 j and -0.5 ± 2.9j (the poles of the free-free beam are -0.0116 ± 1.1643i and -0.0321 ± 3.2094i respectively).

Table 3: Controller design specifications

Position error of $\underline{r}_{Gs}(\Delta t)$	[m]	$\pm$ 0.1
Orientation error of $\theta_s(\Delta t)$	[deg]	$\pm$ 0.05
Residual vibration at beam ends	[m]	$\pm$ 0.03
Residual vibration at robot base	[m]	$\pm$ 0.05

The beam is considered rigid along the X direction and flexible along the Y direction. Therefore, different PI controllers are used to control the X. Y components of $\underline{f}_{si}$: $G_{CFX} = (0.9s + 0.08)/s^2$, $G_{CFY} = (0.8s + 0.5)/s^2$. The gains of the PD controllers for the joint angles of each manipulator are $\underline{K}_{PM}$ = 1000[38 22.7], $\underline{K}_{DM}$ = 1000[14 8.4]. The gains of the PD controller for the motion of the reaction wheel are k_{Pw}=200, k_{Dw}=500. Robots manipulate the beam from the initial position $\underline{r}_{Gs}(0) = \theta_s(0) = 0$ to a final desired position $\underline{r}_{Gs}(\Delta t) = [0 \quad -6]^T$, $\theta_s(\Delta t) = 0$ rad within $\Delta t =$ 40 sec. The errors in the knowledge of the beam inertial and vibration properties are 8%.

5.2. Results

The performance of the AMVM is compared to the performance of a joint PD controller (for the same robot motion trajectories). Fig. 5 shows the position error of the beam CM. Fig. 6 shows the vibration displacement in the left beam end. Fig. 5 and 6 show that AMVM results in small beam positioning errors and low residual vibration in the beam (within the specifications of Table 3). Fig. 5 and 6 also show that the force planning modification compensates the assumed modeling errors and disturbances (without force modification an 8% parameter error in the beam model can result in position errors of 0.5m). On the other hand, PD controlled robots fail to position the beam accurately and with low residual vibration. This poor performance is largely due to the large vibration that robots induce in the LSS, which is caused by the forces that robots apply to the LSS. Joint PD controlled robots cannot control these forces.

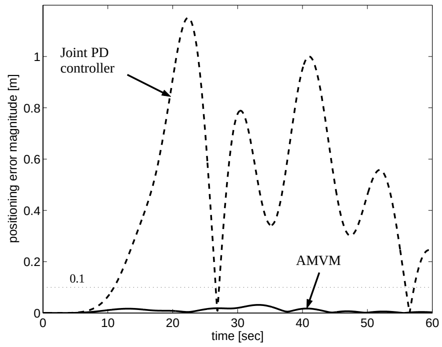

Fig. 5: Position error of the beam CM.

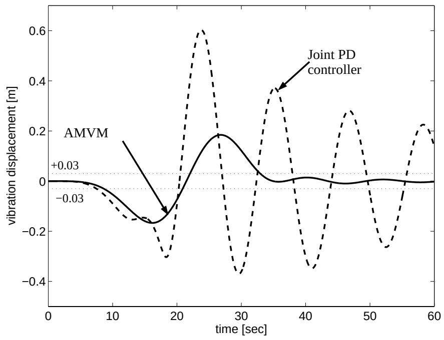

Fig. 6: Vibration displacement in the left beam end.

Fig. 7 shows the Y component of the force $\underline{f}_{b1}$ that robot 1 applies to the LSS. It shows that AMVM controlled robots greatly reduce the forces that they apply to the LSS and therefore induce very small vibration in the LSS, see Fig. 8. AMVM-controlled robots achieve this by using only their end-effector force sensors, eliminating the need to measure the inertial position of their end-effectors, which is difficult in space.

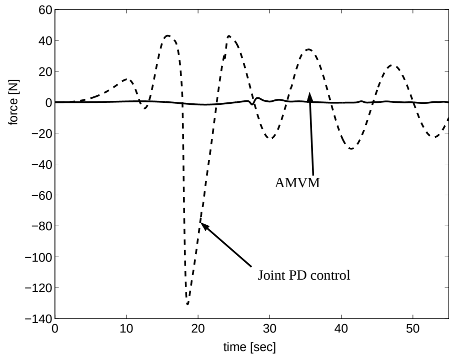

Fig. 7. Y component of the force that robot 1 applies to the LSS.

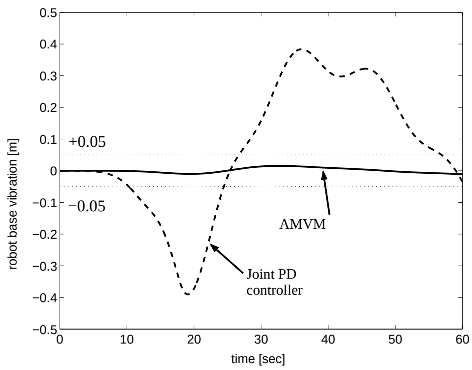

Fig. 8. Vibration displacement of the LSS in the grasping point of robot 1.

Fig. 9 shows the configuration of robot 1 in the beginning and in the end of the manipulation task. It shows that the robot greatly reduces the Y component of the force it applies to the LSS by moving up its CM according to the force that it applies to the module.

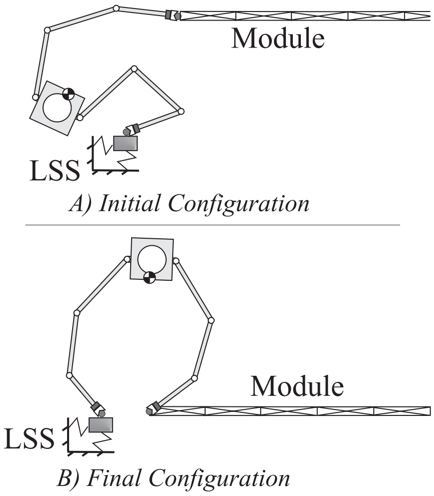

Fig. 9. Configuration of robot 1 in the beginning and the end of the manipulation.

Fig. 10 shows the actuator input in the joint motors and in the reaction wheel motor of robot 1. It shows that motors closer to the robot body need to apply larger torques. The torque applied in the reaction wheel is comparable to the torques applied in the joints. Fig. 11 shows the angular velocity $\dot{\psi}_1$ of the reaction wheel of robot 1. This figure shows that in the end of the maneuver the angular velocity of the reaction wheel approaches zero. While the peak value of $\dot{\psi}_1$ is relatively large, it can be reduced by considering the robot angular momentum in the robot motion planning.

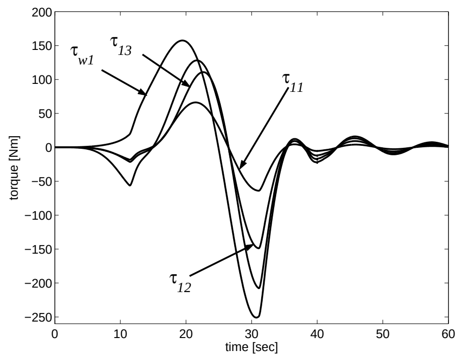

Fig. 10. Applied torque by the joint motors and by the reaction wheel motor of robot 1.

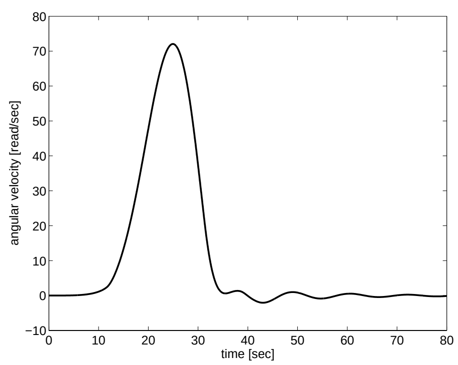

Fig. 11. Angular velocity of robot 1 reaction wheel.

6. CONCLUSION

This paper describes a planning and control architecture (AMVM) for the manipulation of large flexible space structures by teams of space robots. In the architecture developed, robots perform the manipulation task by planning and controlling the forces that they apply to the space structures. Robots exploit their redundancy to improve the force control performance and to avoid collisions. Simulation results for the cooperative manipulation of a large flexible beam by two planar redundant robots show the effectiveness of the architecture in maneuvering the beam accurately while exciting low residual vibration in the beam and the LSS. The results were robust to reasonable modelling errors and external disturbances.

ACKNOWLEDGEMENTS

This work is sponsored by the Japanese Aerospace Exploration Agency (JAXA). Authors would like to thank Prof. Y. Okhami, Prof. M. Oda, H. Ueno, Y. Ishijima, Dr. M. Lichter for their helpful comments.

REFERENCES

Bhat S. and D. Miu (1990), Precise Point-To-Point Positioning Control of Flexible Structures, *ASME Journal of Dynamic Systems Measurement and Control*, **Vol. 112**, no. 4, pp. 667- 674, December 1990.

Gawronski W. (1998), *Dynamics and Control of Structures; a Modal Approach,* Springer Verlag.

Khatib O. (1995), Inertial Properties in Robotic Manipulation: An Object-Level Framework, *The International Journal of Robotics Research*, **vol. 14**, No. 1, pp. 19-36, February 1995.

Lichter M. D. and S. Dubowsky (2005), Shape, Motion and Parameter Estimation of Flexible Space Structures using Laser Rangefinders, *Proc. 2005 IEEE International Conference on Robotics and Automation.*

Oda, M., H. Ueno and M. Mori (2003). Study of the Solar Power Satellite in NASDA. *Proc. I-SAIRAS 2003,* Nara, Japan.

Papadopoulos E. and S. Dubowsky (1991), Coordinated Manipulator/Spacecraft Motion Control for Space Robotic Systems, *Proc. 1991 IEEE International Conference on Robotics and Automation.*

Meirovich L. (1970), *Methods of Analytical Dynamics*, Dover Publications, New York.

Nakamura Y. (1991), *Advanced Robotics; Redundancy and Optimization*, Addison Wesley Publishing.

Vafa Z. and S. Dubowsky (1987), On the Dynamics in Space Using the Virtual Manipulator Approach, *Proc. 1987 IEEE International Conference on Robotics and Automation.*

Whittaker W., et al. (2000), Robotics for Assembly, Inspection, and Maintenance of Space Macrofacilities, *Proc. AIAA Space 2000 Conf.*